SUPPLEMENTAL MATERIAL

Figure S1. WORLD OCEAN FLOOR SEDIMENTS. Map of seabed sediments from Dutkiewicz et al. (2015), showing that calcareous ooze occupies a significant portion (c. 30%) of seafloor. Thus, it is important to study its behaviour during remobilisation through submarine landsliding.

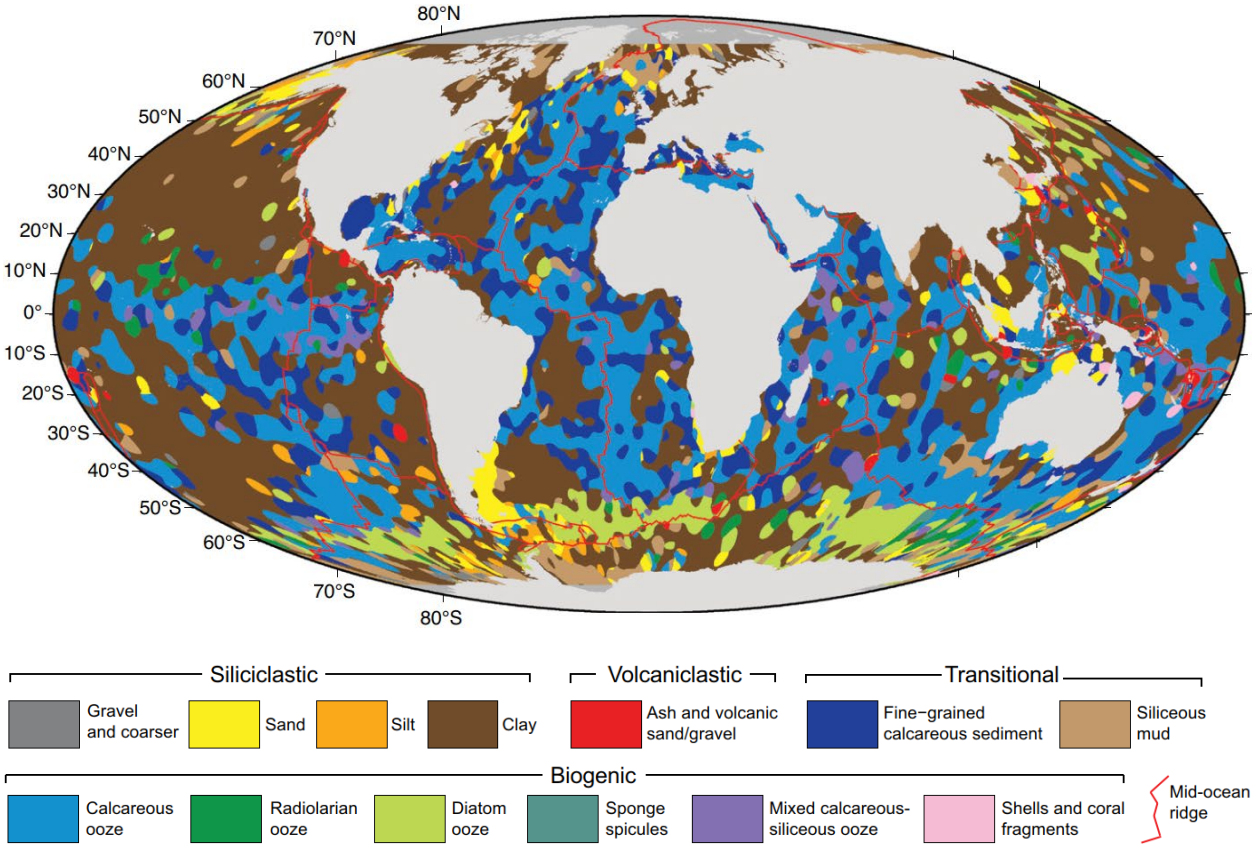

References for Figure S1

Dutkiewicz, A., Müller, R. D., O'Callaghan, S., and Jónasson, H., 2015, Census of seafloor sediments in the world's ocean: Geology, v. 43, no. 9, p. 795-798.

TABLE S1. LIST OF SEISMIC AND WELL DATA PROVIDED BY GEOSCIENCE AUSTRALIA (https://www.nopims.gov.au/)

A list of seismic reflection data and their properties used in this study.

No	Survey Name	Vintage	Bin Size (m)		Dominant Frequency* (Hz)	Vertical Resolution (m)
			Xline	Inline		
1	Acme 3D	2006	18.75	25	40	11
2	Draeck 3D	2006	18.75	25	40	11
3	Duyfken 3D	2006	12.5	18.75	50	9
4	Gorgon 3D	1992	20	25	40	11
5	Io-Jansz 3D	2005	18.75	12.5	60	8

**Dominant frequency at basal-shear surface (base of MTC) level.*

A list of well data and used in this study. Velocity and lithology data are from well reports.

No	Well name	Water velocity (m/s)	Near seabed sediments velocity (m/s)	Lithology
1	Bluebell-1	1524	-	-
2	Central Gorgon-1	1524	-	-
3	Chrysaor-1	1524	-	-
4	Gorgon-1	1524	-	-
5	North Gorgon-1	1524	-	-
6	Clio-1	1500	-	-
7	Orthrus-1	1500	-	-
8	Io-1	1524	-	-
9	Jansz-1	1524	-	-
10	Jansz-3	1524	-	-
11	ODP 762	-	1824	Foraminifer ooze

FIGURE S2. INSIGHTS ON OVERALL EMPLACEMENT PROCESSES FROM VD/VE RATIO

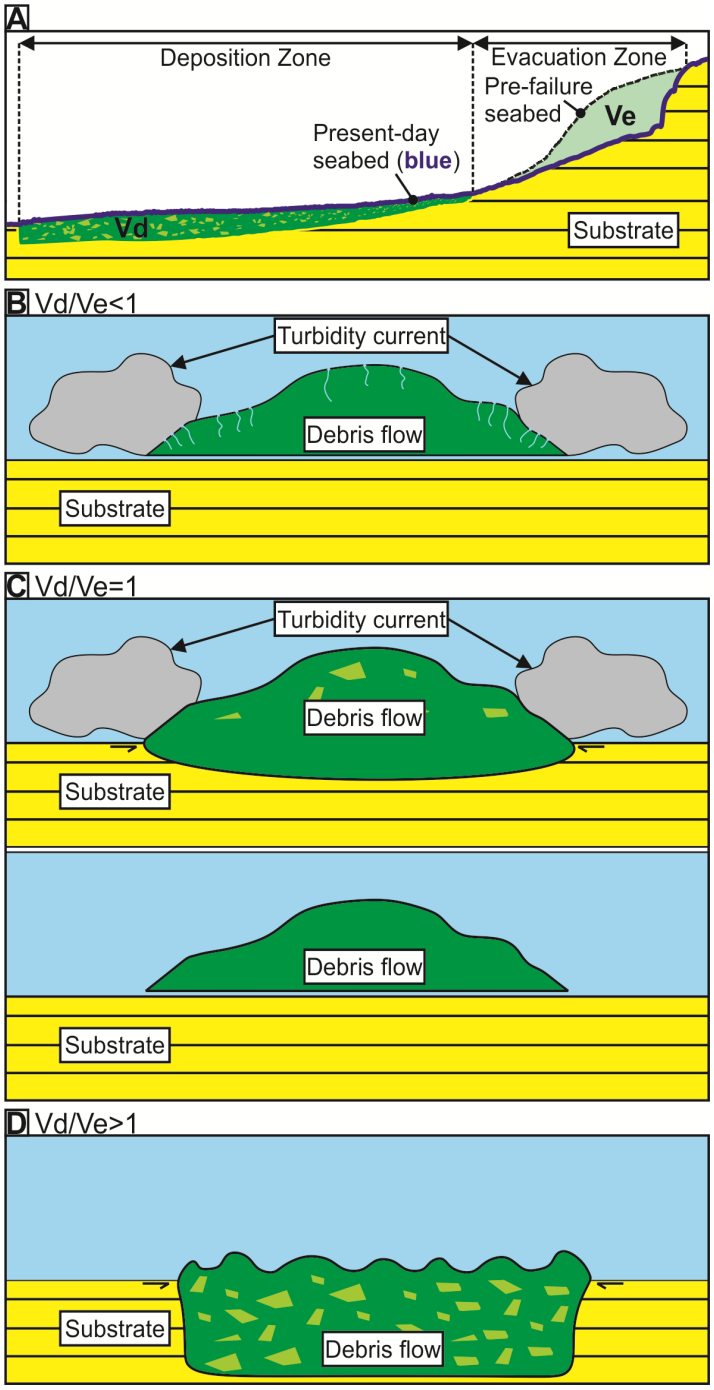

A: An illustration of evacuated volume (Ve), volume of sediment between pre-failure and present-day seabed, in the evacuation zone; and deposited volume (Vd), between base and top (present-day seabed) of a submarine landslide, in the deposition zone. We then use Vd/Ve ratio as a first-degree estimation of erosion by the submarine landslide, from which we suggest three hypothesis (B-D).

B: Vd/Ve<1 implies that Vd<Ve, suggesting volume loss during emplacement.

C: Vd/Ve=1 implies that Vd=Ve, either minor erosion balanced by partial flow transformation from debris flow to turbidity current (top), or hydroplaning during emplacement (overriding debris flow is separated from underlying substrate by a thin lubricating layer) (bottom).

D: Vd/Ve>1 implies that Vd>Ve, suggesting substrate entrainment and erosion during transport.

TABLE S2. VOLUME CALCULATION METHODS.
Three volume calculation methods used to calculate Ve and Vd of the Gorgon Slide.

Methodology	Volume Calculation	Uncertainties	References
Bulk volume	Ve is estimated by calculating the volume between present-day and interpreted pre-failure seabed within the evacuation zone Vd is obtained by calculating the volume of the deposit between the basal-shear surface and top surface	Related to **seismic interpretation**	e.g. Piper et al. (1997); Sun et al. (2018)
Compacted volume	Similar approach to bulk volume method, but counts only the solid-state sediment fraction, removing water and pore-space (i.e. theoretical zero-porosity) *Compacted Ve (Vec)* $Vec = Ve\ x\ (100 - porosity)/100$ *Compacted Vd (Vdc)* $Vdc = Vd\ x\ (100 - porosity)/100$	The same as the bulk volume, but include **porosity estimation**	e.g. Lamarche et al. (2008)
Theoretical volume	Ve is assumed as a wedge-shaped geometry *Ve = ½ x area x scarp height* Vd is assumed as a half-ellipsoid geometry *Vd:* $\frac{1}{6}\pi$ *x thickness x width x length*	**Oversimplified geometry**	e.g. McAdoo et al. (2000) e.g. Wilson et al. (2004)

An illustration of the three volume calculation methods used to calculate Ve and Vd of the Gorgon Slide.

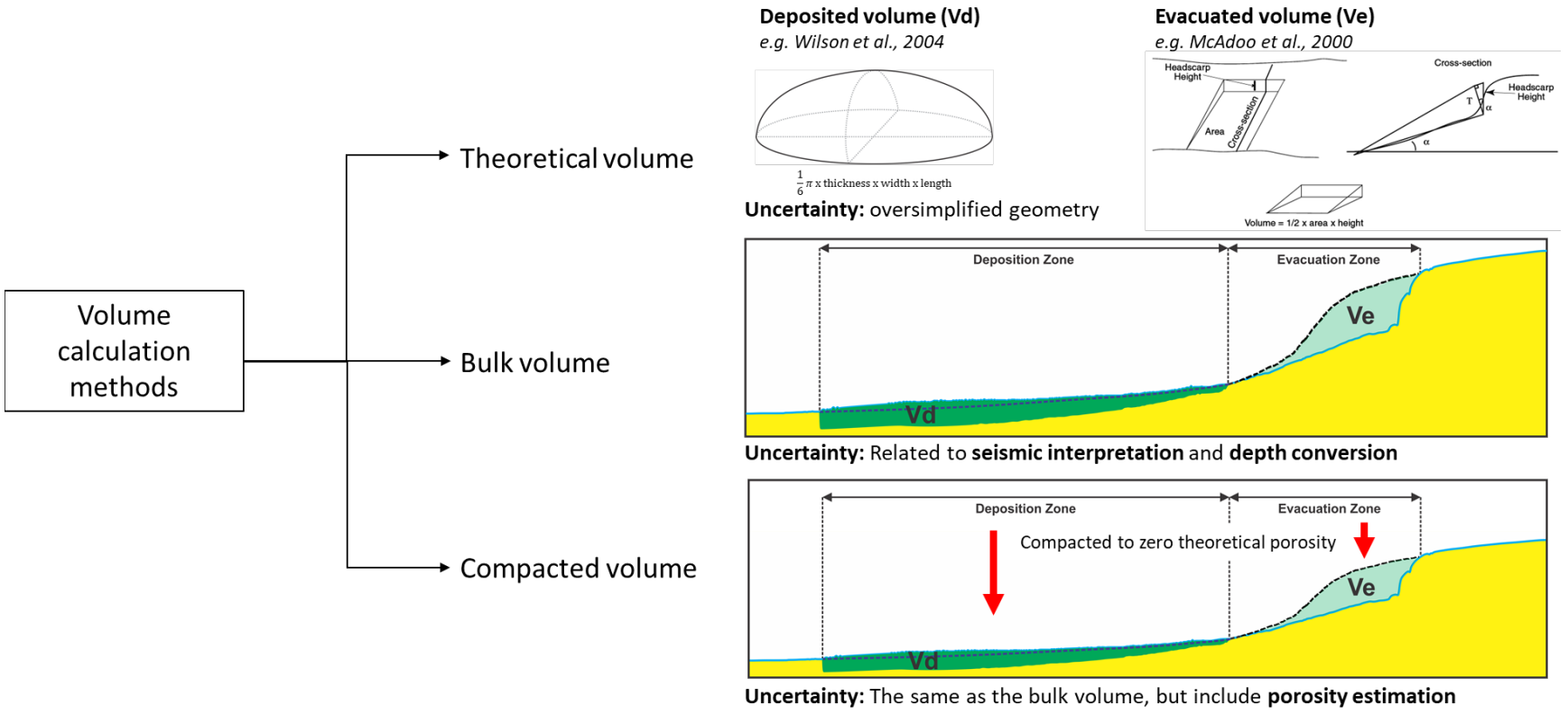

References for Table S2

Lamarche, G., Joanne, C., and Collot, J. Y., 2008, Successive, large mass-transport deposits in the south Kermadec fore-arc basin, New Zealand: The Matakaoa Submarine Instability Complex: Geochemistry, Geophysics, Geosystems, v. 9, no. 4.

McAdoo, B., Pratson, L., and Orange, D., 2000, Submarine landslide geomorphology, US continental slope: Marine Geology, v. 169, no. 1, p. 103-136.

Piper, D. J. W., Pirmez, C., Manley, P. L., Long, D., Flood, R. D., Normark, W. R., and Showers, W., Mass Transport Deposits of the Amazon Fan, *in* Proceedings Ocean Drilling Program, Scientific Results1997, Volume 155, p. 109-146.

Sun, Q., Alves, T., Lu, X., Chen, C., and Xie, X., 2018, True volumes of slope failure estimated from a Quartenary mass-transport deposit in the northern South China Sea: Geophysical Research Letters.

Wilson, C. K., Long, D., and Bulat, J., 2004, The morphology, setting and processes of the Afen Slide: Marine Geology, v. 213, no. 1-4, p. 149-167.

FIGURE S3. VOLUME BALANCE OF THE GORGON SLIDE. Evacuated volume calculation (for bulk and compacted volume methods) used two interpretations of reconstructed slope as minimum (A-B) and maximum (B-C) estimates.

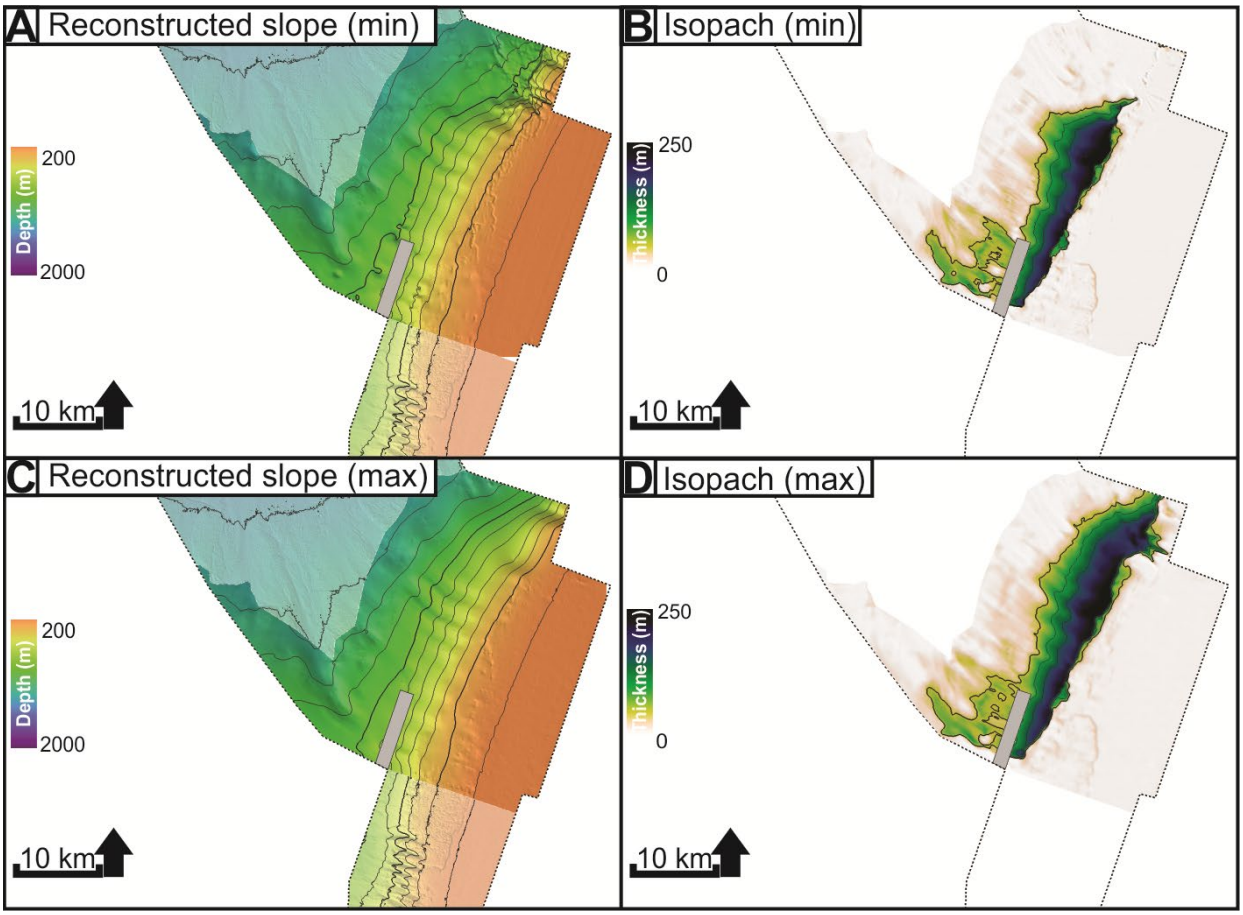

Calculated Vd and Ve of the Gorgon Slide using the three methods.

Minimum estimate (Fig. DR5A-B)

Methods	Ve (km^3)	Vd (km^3)	Vd/Ve
Bulk	31	509	**16.4**
Compacted	19	255	**13.4**
Theoretical	115	550	**4.8**

Maximum estimate (Fig. DR5C-D)

Methods	Ve (km^3)	Vd (km^3)	Vd/Ve
Bulk	43	509	**11.8**
Compacted	26	255	**9.8**
Theoretical	115	550	**4.8**

The Gorgon Slide Morphometry	
Evacuation area (km^2)	656
Deposition area (km^2)	1760
Scarp height (m)	350
Max. thickness (m)	500
Length (km)	70
Width (km)	30

Porosity assumption*	
ODP 762 near seabed sediments (>371 mbsf)	39
Redeposited chalk	50

**Near seabed sediments porosity is from ODP 762 data (see O'Brien and Manghnani, 1992) . Redeposited chalk could have porosity of 50-55% at time of deposition, prior to be buried (Hardman, 1982). This is in contrast with fine-grained siliciclastics, where redeposited sediments would have lower porosity than that of in-situ sediments (e.g. Sun et al., 2018).*

References for Figure S3

Hardman, R., 1982, Chalk reservoirs of the North Sea: Bulletin of the Geological Society of Denmark, v. 30, no. 3-4, p. 119-137.

O'Brien, D., and Manghnani, M., 1992, Physical properties of Site 762: a comparison of shipboard and shore-based laboratory results. In von Rad, U., Haq, BU, et al, *in* Proceedings Proc. ODP, Sci. Results 1992, Volume 122, p. 349-362.

Sun, Q., Alves, T., Lu, X., Chen, C., and Xie, X., 2018, True volumes of slope failure estimated from a Quartenary mass-transport deposit in the northern South China Sea: Geophysical Research Letters.

TABLE S3. A LIST OF SUBMARINE LANDSLIDES ACROSS THE GLOBE USED IN THIS STUDY

Name	Area (km^2)	Height Drop (m)	Length (km)	H/L	Thickness (m)	Volume Evacuated (km^3)		Volume Deposited (km^3)		Vd/Ve	Vd/Ve Min	Vd/Ve Max	Composition	Geological Setting	Reference
Ruatoria Debris Avalanche	3400	3200	62	0.052	1300	2570	±514	1958	±392	0.76	0.61	0.91	Mixture	Convergent Margin	Collot et al., 2001
MTD South China Sea	11100	2800	330	0.008	150	715	-	629	±36	0.88	0.83	0.93	Siliciclastic	Passive Margin	Sun et al., 2018
Gebra Slide_A	280	450	70	0.006	175	20	-	21	-	1.05	-	-	Mixture	Extensional Margin	Imbo et al., 2003
Afen Slide Stage 1	48	290	12	0.024	8	0.126	-	0.142	-	1.13	-	-	Siliciclastic	Passive Margin (Glacial)	Wilson et al., 2004
Nataraja Slide	49000	3150	550	0.006	330	11000	-	19000	±4000	1.73	1.36	2.09	Mixture	Passive Margin	Calves et al., 2015
Angola MTD	430	-	30	-	200	10	-	20	-	2.00	-	-	Siliciclastic	Passive Margin	Gee et al., 2006
WMTD Amazon	10000	3000	245	0.012	150	650	±150	2000	-	3.08	2.50	4.00	Siliciclastic	Passive Margin	Piper. et al., 1997
Viper Slide	18.7	160	5.5	0.029	31	0.025	-	0.099	-	3.96	-	-	Mixture (siliciclastic and carbonate)	Passive Margin	Webster et al., 2016
Brunei Slide	5300	2300	120	0.019	240	240	-	1200	±12	5.00	4.95	5.05	Siliciclastic	Transpressive Margin	Gee et al., 2007
Matakaoa Debris Flow (MDF)	10000	2050	200	0.010	300	140	±40	1050	±100	7.50	6.79	8.21	Siliciclastic	Convergent Margin	Joanne et al., 2013
Gondola Slide (G1-MTD)	1050	955	55	0.017	50	4.3	-	40	-	9.30	-	-	Siliciclastic (muddy deposits)	Convergent Margin	Dalla Valle et al., 2015
Gorgon Slide	1593	1000	65	0.015	500	19	-	255	-	13.4	4.79	16.4	Carbonate (foraminifer nannofossil ooze)	Passive Margin	Nugraha et al. (*this study*)

References for Table S3

Calvès, G., Huuse, M., Clift, P. D., and Brusset, S., 2015, Giant fossil mass wasting off the coast of West India: the Nataraja submarine slide: Earth and Planetary Science Letters, v. 432, p. 265-272.

Collot, J. Y., Lewis, K., Lamarche, G., and Lallemand, S., 2001, The giant Ruatoria debris avalanche on the northern Hikurangi margin, New Zealand: Result of oblique seamount subduction: Journal of Geophysical Research: Solid Earth, v. 106, no. B9, p. 19271-19297.

Dalla Valle, G., Gamberi, F., Foglini, F., and Trincardi, F., 2015, The Gondola slide: a mass transport complex controlled by margin topography (South-Western Adriatic Margin, Mediterranean Sea): Marine Geology, v. 366, p. 97-113.

Gee, M., Gawthorpe, R., and Friedmann, S., 2006, Triggering and evolution of a giant submarine landslide, offshore Angola, revealed by 3D seismic stratigraphy and geomorphology: Journal of Sedimentary Research, v. 76, no. 1, p. 9-19.

Gee, M., Uy, H., Warren, J., Morley, C., and Lambiase, J., 2007, The Brunei slide: a giant submarine landslide on the North West Borneo Margin revealed by 3D seismic data: Marine Geology, v. 246, no. 1, p. 9-23.

Imbo, Y., De Batist, M., Canals, M., Prieto, M., and Baraza, J., 2003, The Gebra slide: a submarine slide on the Trinity Peninsula Margin, Antarctica: Marine Geology, v. 193, no. 3-4, p. 235-252.

Joanne, C., Lamarche, G., and Collot, J. Y., 2013, Dynamics of giant mass transport in deep submarine environments: the Matakaoa Debris Flow, New Zealand: Basin Research, v. 25, no. 4, p. 471-488.

Piper, D. J. W., Pirmez, C., Manley, P. L., Long, D., Flood, R. D., Normark, W. R., and Showers, W., Mass Transport Deposits of the Amazon Fan, *in* Proceedings Ocean Drilling Program, Scientific Results1997, Volume 155, p. 109-146.

Sun, Q., Alves, T., Lu, X., Chen, C., and Xie, X., 2018, True volumes of slope failure estimated from a Quartenary mass-transport deposit in the northern South China Sea: Geophysical Research Letters.

Webster, J. M., George, N. P., Beaman, R. J., Hill, J., Puga-Bernabéu, Á., Hinestrosa, G., Abbey, E. A., and Daniell, J. J., 2016, Submarine landslides on the Great Barrier Reef shelf edge and upper slope: A mechanism for generating tsunamis on the north-east Australian coast?: Marine Geology, v. 371, p. 120-129.

Wilson, C. K., Long, D., and Bulat, J., 2004, The morphology, setting and processes of the Afen Slide: Marine Geology, v. 213, no. 1-4, p. 149-167

FIGURE S47. RELATIONSHIP BETWEEN EROSIVITY AND OTHER SLIDE PARAMETERS

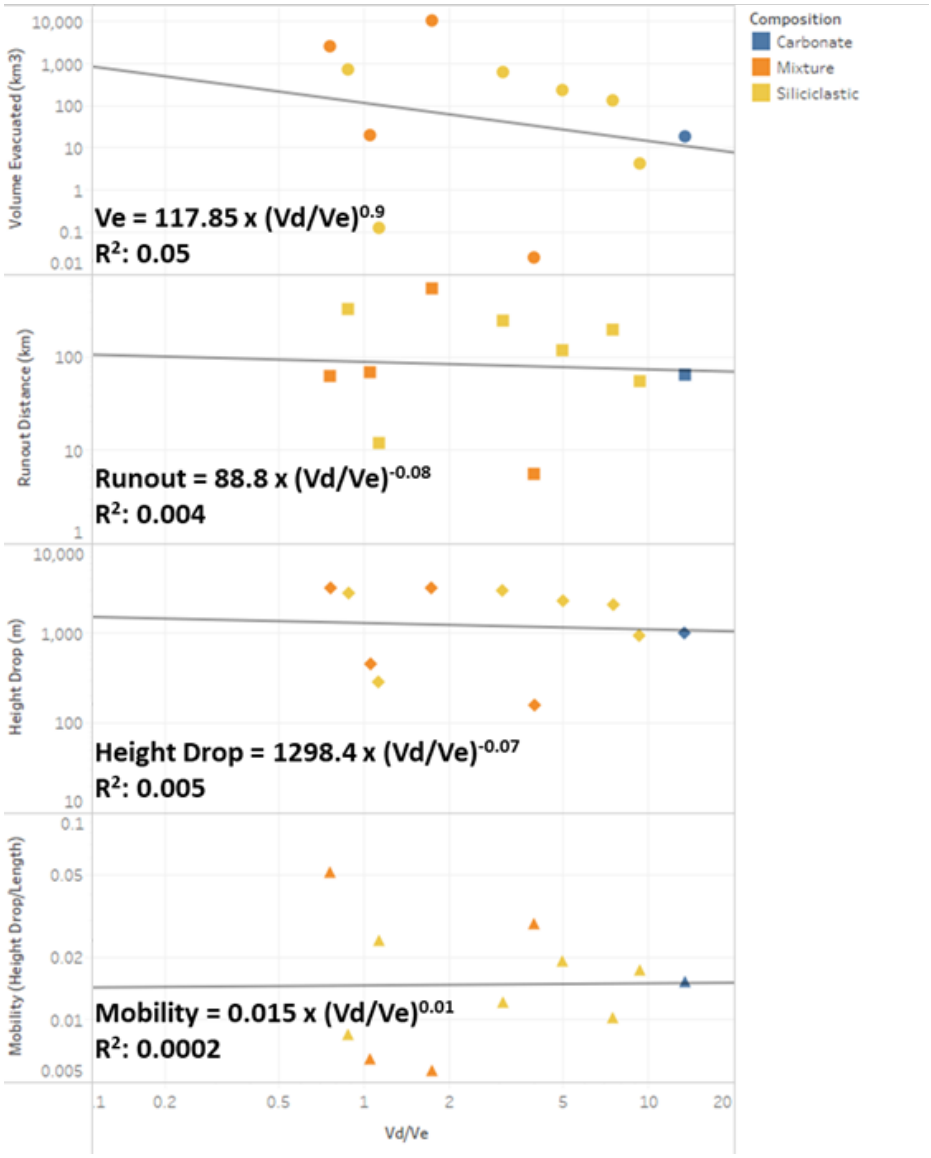

We found no clear relationship found between erosivity (Vd/Ve ratio) and those parameters. This suggests that they may have limited predictive power, and thus local factors influencing transport processes (such as topography variation) are at play.

FIGURE S8. GEOTECHNICAL BEHAVIOUR OF CARBONATE OOZE, OFFSHORE NW AUSTRALIA. Strength degradation of sediments during cyclic T-bar test (modified from Gaudin and White, 2009). The Y axis is a ratio of remoulded over initial shear strength, and the X axis is the number of T-bar cycles. It can be seen that West African Clay (diatomaceous sediments from offshore Angola) have a residual post-failure strength that is c. 55% of the initial shear strength, compared to carbonate silts from deepwater NW Australia that can be as low as 10%.

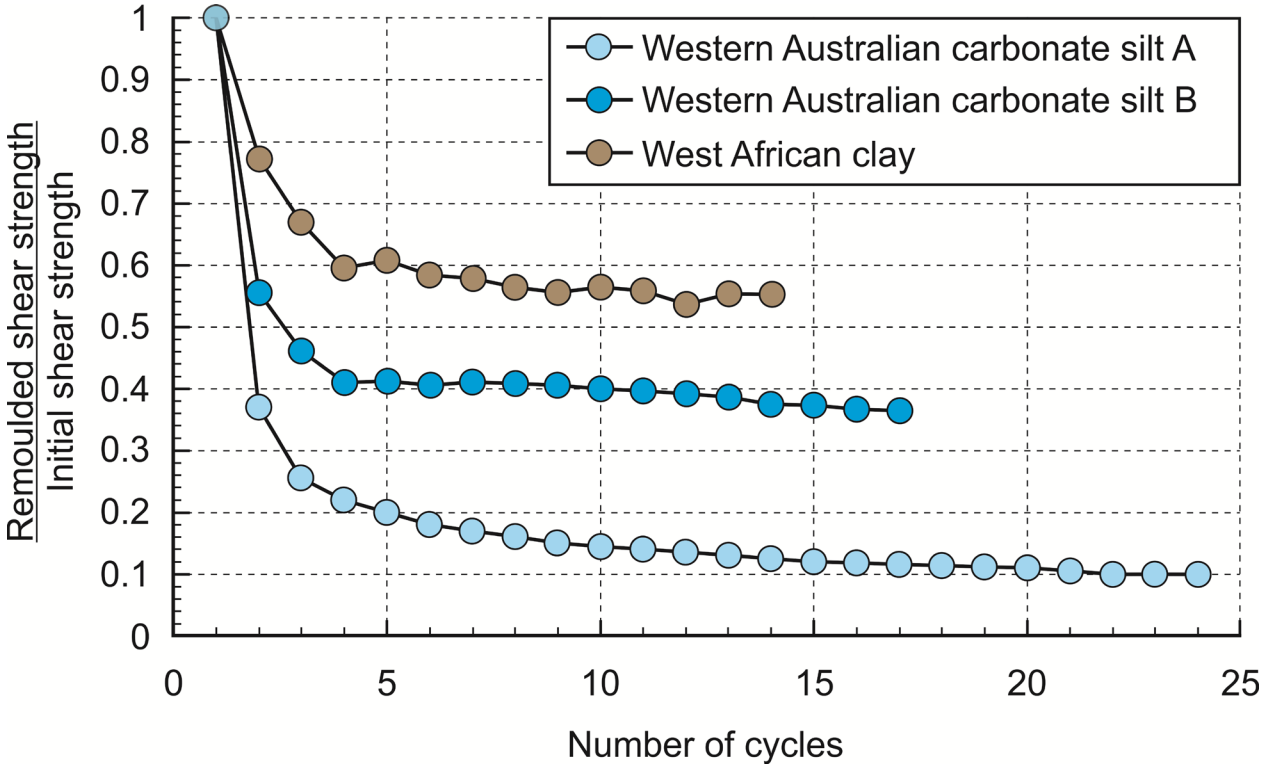

References for Figure S8

Gaudin, C., and White, D., 2009, New centrifuge modelling techniques for investigating seabed pipeline behaviour, *in* Proceedings 17th International Conference on Soil Mechanics and Geotechnical Engineering, Alexandria, 2009, p. 448-451.